

Experimental study on shear performance of partially precast Castellated Steel Reinforced Concrete (CPSRC) beams

Yong Yang^{*1}, Yunlong Yu¹, Yuxiang Guo¹,
Charles W. Roeder³, Yicong Xue¹ and Yongjian Shao²

¹ School of Civil Engineering, Xi'an University of Architecture & Technology, Xi'an, Shannxi 710055, China

² Suzhou University of Science & Technology, Suzhou, Jiangsu 215009, China

³ Civil and Environmental Department, University of Washington, Seattle, WA 98115, USA

(Received December 17, 2015, Revised March 25, 2016, Accepted March 29, 2016)

Abstract. A new kind of partially precast or prefabricated castellated steel reinforced concrete beam, which is abbreviated here as CPSRC beam, was presented and introduced in this paper. This kind of CPSRC beam is composed of a precast outer-part and a cast-in-place inner-part. The precast outer-part is composed of an encased castellated steel shape, reinforcement bars and high performance concrete. The cast-in-place inner-part is made of common strength concrete, and is casted with the floor slabs simultaneously. In order to investigate the shear performance of the CPSRC beam, experiments of six CPSRC T-beam specimens, together with experiments of one cast-in-place SRC control T-beam specimen were conducted. All the specimens were subjected to sagging bending moment (or positive moment). In the tests, the influence of casting different strength of concrete in the cross section on the shear performance of the PPSRC beam was firstly emphasized, and the effect of the shear span-to-depth ratio on that were also especially taken into account too. During the tests, the shear force-deflection curves were recorded, while the strains of concrete, the steel shapes as well as the reinforcement stirrups at the shear zone of the specimens were also measured, and the crack propagation pattern together with the failure pattern was as well observed in detail. Based on the test results, the shear failure mechanism was clearly revealed, and the effect of the concrete strength and shear span-to-depth ratios were investigated. The shear capacity of such kind of CPSRC was furthermore discussed, and the influences of the holes on the steel shape on the shear performance were particularly analyzed.

Keywords: steel reinforced concrete structure; precast steel reinforced concrete beam; castellated steel shape; shear performance; shear capacity; experimental study

1. Introduction

As mentioned in the reference paper (Hong *et al.* 2009, 2010), a new construction approach which was named of partially precast SRC structure and abbreviated as PPSRC structure was proposed and introduced. In the reference paper, the cross section form, and the constitution details as well as the construction methods of this kind of PPSRC beam were introduced in detail, together with a series of experiments on the shear performance of the PPSRC beam.

As well known, since the 1950s, because the high strength to weight ratio of castellated beams

*Corresponding author, Professor, E-mail: yhhp2004@163.com

has been an asset to structural engineers in their efforts to design more lighter and more cost efficient steel structures, the castellated steel shapes were used widely (Johnson 2004, Chen and Jia 2008). The strength to weight ratio of the castellated steel shape is higher than that of the common steel shape, especially in bearing bending moment. For an example illustrated in Fig. 1, when a common steel shape was transformed to a castellated steel shape, the depth of the steel shape could become 1.5 times larger than before, which could result in almost 1.5 times larger in flexural capacity too. Except that such attractive merit of high flexural capacity to weight, there were also some problems or shortcoming in it. Firstly, the shear capacity of the castellated steel shape is challenged due to a series of large holes on the web of the castellated steel shapes, which were supposed to weaken the shear capacity. Secondly, the problem of the local buckling of the web also comes to be concerned, especially when the web is at the compression zone (Leon 2004, 2008, Chen *et al.* 2015).

In order to overcome these two problems, a concept of encasing the castellated steel shape in precast concrete was proposed, and then a new kind of precast castellated steel reinforced concrete beam, which was abbreviated as CPSRC beam, was formed. As illustrated in Fig. 2, the castellated steel shape, together with some reinforcing bars and high performance concrete, was precast or prefabricated in shops to form a precast outer-part of the beam. After that, the outer-part was transported to the construction site and set-up as planned, where it could act as formworks for another inner-part concrete and the adjacent floor slabs casted-in-place afterwards. The precast outer-part was supposed to combine well with the cast-in-place part to form a complete cross section, then the CPSRC beams was formed.

In such kind of CPSRC beams, because the castellated steel shape was encased or wrapped in the concrete, the local buckling problems were easily avoided (Yang *et al.* 2012). Furthermore, the problem of weakness in shear capacity was supposed to be compensated or enhanced by the web

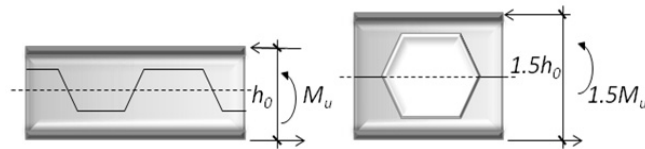


Fig. 1 The schematic diagram of the castellated steel shape beam

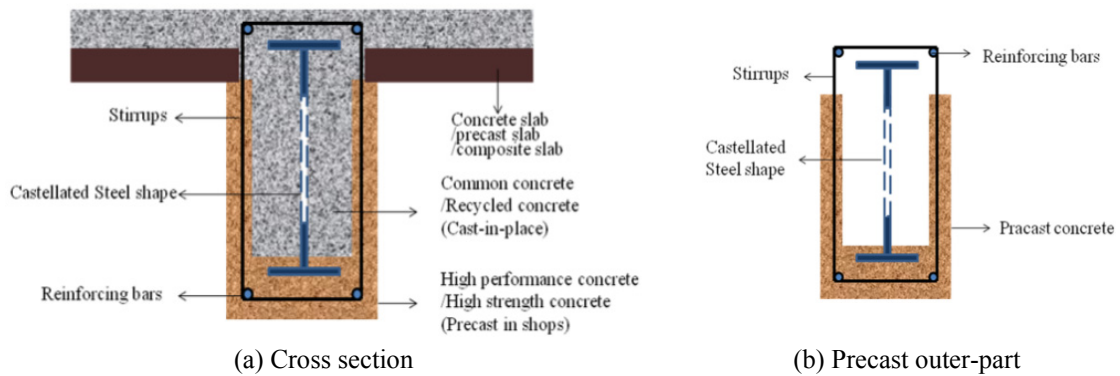


Fig. 2 The schematic diagram of the CPSRC beam

concrete (Nie *et al.* 2004). Therefore, two main problems caused by the castellated steel shape were fulfilled. And as mentioned above, the first of some important benefits of this kind of CPSRC beam is much less cost in steel material due to the high capacity to weight ratio of the castellated steel shape. The second important merit of the CPSRC beam is less cost in the labor time during the in-site construction stage, because most of works such as fabricating and erecting the steel shape, tying-up the reinforcing bars and casting the outer-part concrete were completed in shops, and moreover there was always no need of the formworks even in shoring works with the help of the precast outer-part. Therefore, the CPSRC beams could be both efficient and eco-friendly.

For the mechanical performance of this kind of CPSRC beams, the flexural performance was supposed to be easily figured out, provided that there were enough interaction between the outer-part and inner-part as well as enough sufficient composition interaction between the castellated steel shape and the concrete in the outer-part, which was already verified by former research experiments. But the shear performance was relatively complicated due to the holes in the web of the castellated steel shape (Lawson *et al.* 2006, Hegger *et al.* 2009, Redwood and Demirdjian 1998). Because not only the size but also the position of the holes was supposed to affect the shear capacity of the steel shape, which was supposed to account for a large portion of the total shear capacity in it.

In order to investigate shear performance of the CPSRC beam, experiments of six CPSRC specimens and one cast-in-place CSRC specimen were conducted. The specimens were all designed as T-beams to test under positive moment or sagging moment. In the tests, the influence of concrete grades was firstly emphasized, while the effect of the shear span-to-depth ratio of the specimens was as well concerned. During the tests, the shear force-deflection curves were recorded, while the strains of concrete and the steel shape as well as the reinforcement stirrups at the shear zone of the specimens were also measured, and the crack propagation patterns together with the failure pattern were as well observed in detail. From the test results, the shear failure mechanism was clearly studied, and the effect of the concrete strength and that of the shear span-to-depth ratios were carefully investigated. The shear capacity of such kind of CPSRC was furthermore discussed, and the influences of the holes in the steel shape on the shear performance were particularly analyzed. Finally, from the comparison between the test results of ten CPSRC beam specimens and that of one control cast-in-place SRC specimen which was cast in place, it could be concluded that the shear performances of CPSRC beams were as good as that of the cast-in-place SRC beam.

2. Test program

2.1 Test specimens

There were a total of seven specimens, which included six CPSRC beam specimens and a cast-in-place CSRC control specimen, all the key parameters of them were listed in the Table 1. All these seven specimens were T-beams with flanges, with the aim to simulate the real floor beams with adjacent slabs in both two sides. All the seven specimens were subjected to sagging moment in the test, and the flanges were supposed to be in compression zone. With these specimens, the shear performances such as the failure pattern as well as the shear capacity were expected to figure out.

2.1.1 Cross sections

These seven T-beam specimens were all the same in the cross section form and the cross

section dimensions except the concrete strength grades. As illustrated in Fig. 3, the depth of the whole cross section was 400 mm, both the height and the width of the web in the T-beams were 200 mm, and the width and the thickness of the flange were 880 and 100 mm, respectively.

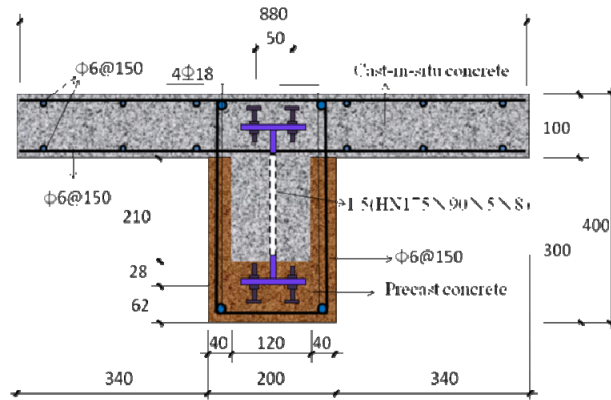
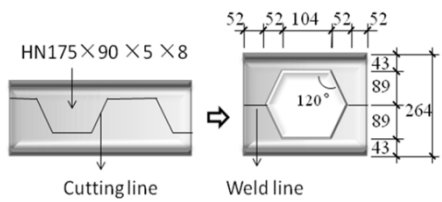
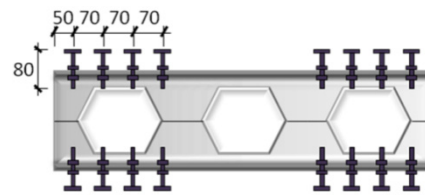


Fig. 3 Schematic diagram of specimens



(a) The schematic and details of the holes



(b) The schematic of the bolts connectors



(c) After cutting



(d) Before welding



(e) After welding

Fig. 4 Prefabrication of the castellated steel shape

The castellated steel shape in every specimen was transformed from the steel shape classified as HN175×90×5×8, based on the classification standards in China, and the strength grade of the the steel shape was Q235, which was graded in Chinese steel standard (GB/T 700-2006), the nominal yield strength of the steel shape was 235 MPa. Before the transformation, the total depth and width of the steel shape HN175×90×5×8 were 175 mm and 90 mm, and the thickness of the web and flanges were 5 mm and 8 mm respectively. As illustrated in Fig. 1, the castellated steel shape was transformed by welding two parts of steel shape, which were cut from the steel shape HN175×90×5×8 along the designated line. The depth of the castellated steel shape was 262.5 mm, which was 1.5 times of that before transforming, and the details of the castellated steel shape were illustrated in Fig. 4. Instead of using studs as shear connectors, high strength bolts connectors were adopted as shear connectors to transfer the shear force on the interface, which made the fabrication of the specimens much easier. The bolts connectors were located both in the top flange and the bottom flanges of the steel shape. The diameter and the length of the bolts connectors were 12 mm and 80 mm, respectively. The arrangements of the bolts were illustrated in both Figs. 3 and 4. The bolts passed through the holes of the flanges, which can transfer the shear force of both two sides of the flanges.

2.1.2 Materials

As mentioned above, the steel shapes of all the specimens were the same grade, which was HN175×90×5×8. For the flanges of the steel shape, the tested tensile strength was 273 MPa (39,585 psi) at yield and 450 MPa (65,250 psi) at failure, respectively, while for the web of the steel shape, the tested tensile strength was 262 MPa at yield and 436 MPa at peak, respectively. The tested tensile strength of the stirrups, Ø6 bars with the diameter of 6 mm with the grade of HRB335, was 387 MPa at yield and was 545 MPa at peak, while the tested tensile strength of the longitudinal reinforcements, Ø20 bars with the diameter of 20 mm and with the grade of HRB400, was 420 MPa at yield and was 578 MPa at peak.

The concrete strength was determined by compression tests of concrete cubic specimens, which was according to the Chinese standards (GB/T50081-2002). The size of the tested cubic specimens is 150×150×150 mm, and the cubic specimens strength was natural cured for 28 days before the compression test. The strength grades of concrete in the outer-part and the inner-part in the CPSRC specimens were different. For six PPSRC specimens here, the strength grade of concrete

Table 1 Matrices of test specimens

Specimen ID	Effective depth of section d (mm)	Shear span length a (mm)	Shear span-to-depth ratios a/d	Cubic compression strength of outer-part concrete $f_{c,out}$ (MPa)	Cubic compression strength of inner-part concrete $f_{c,in}$ (MPa)	Test setup
CPSRC-1	365	365	1.0	54.0	21.7	three-point test
CPSRC-2		550	1.5	54.0	21.7	four-point test
CPSRC-3		365	1.0	54.0	38.1	three-point test
CPSRC-4		550	1.5	54.0	38.1	three-point test
CPSRC-5		730	2.0	54.0	38.1	three-point test
CPSRC-6		915	2.5	54.0	38.1	three-point test
CPSRC-7		550	1.5	54.0	68.0	four-point test

of the outer-part was designed to be C60 graded under the Chinese codes (GB/T 50081-2002), having the test cubic compressive strength of 54.0 MPa at 28 days period. The strength grades of concrete in the inner-part were designed in three levels, C20, C40 and C60 respectively, and the tested cubic compressive strengths of the concrete of C20, C40, and C60 at 28 days were 21.7 MPa, 38.1 MPa and 68.0 MPa respectively, which were all illustrated in Table 1.

2.2 Test setup and instrumentations

In the experiment, all the specimens were tested on an electro hydraulic servo-testing machine, whose maximum capacity is 5000 kN. As illustrated in Fig. 5, five specimens were loaded in three-point test, and two specimens CPSRC-2 and CPSRC-6 were loaded in four-point test.

Static loads were applied at the loading point by the electro hydraulic servo-controlled hydraulic jacks as denoted in Fig. 5. During the test process, all the deflections of the specimens at the central point, the loading points and the two supports were measured by LVDTs, and from which the shear force-deflections curves and data were be recorded.. The layout of LVDTs was presented in Fig. 4 in detail. Fig. 5 showed the holes position of castellated steel shape in shear span region.

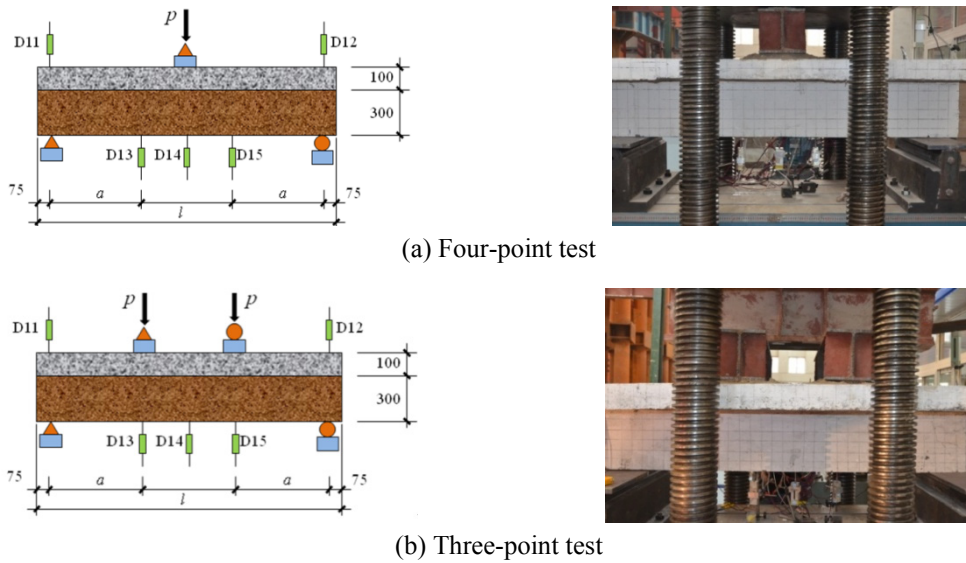
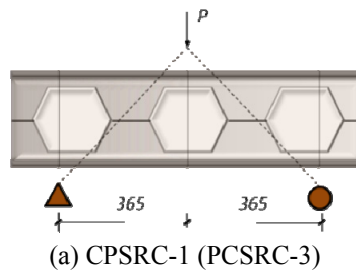


Fig. 5 Schematic diagram and photo of test setup of two series specimens



(a) CPSRC-1 (PCSRC-3)

Fig. 6 Schematic diagram of the location of hexagon hole castellated in shear span region

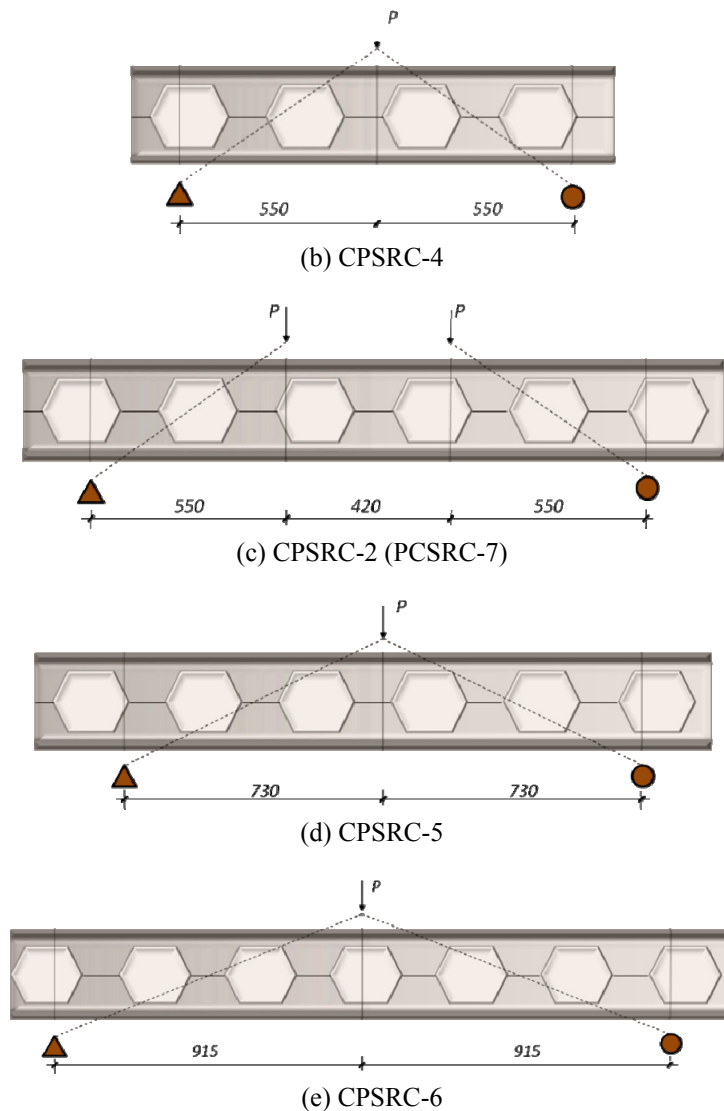


Fig. 6 Continued

3. Test results

3.1 Failure modes and damage patterns

The failure modes or the damage patterns of the typical specimens were shown in Fig. 6, respectively. As illustrated in Fig. 6, five of all the specimens, except the specimen CPSRC-5 and specimen CPSRC-6, failed in typical shear compression failure mode. As a typical example of the specimens subjected to three-point test and failed in shear compression failure mode, the crack propagation process of specimen CPSRC-1 was described as follows. When the total load was 230 kN, the first crack occurred at the tension zone of the load-point section, it was a typical flexural

crack and headed vertically then paused at the height of 20 mm, where the flange of the steel shape was. When the load was up to 330 kN, an inclined crack occurred at the left half of the specimens, which originated from the support and headed to the load-points, and quickly propagated at the bottom of the flange in the T-beam. With the load increasing, a couple of fine inclined cracks occurred, and an inclined crack occurred at the right half of the specimen when the total load was increased to 600 kN, which also originated from the support to the load-point directly with several tiny inclined cracks. With the further increasing of the load, some tiny cracks developed and propagated to large inclined cracks in shear zones. When the total load was up to 1170 kN, the concrete in the flange was crushed and the specimen was supposed to fail since the total load decreased quickly accompanied with the increase of deflections. The crack propagation processes of the five specimens were similar to the specimen CPSRC-1. For the specimen CPSRC-5 and specimen CPSRC-6, whose shear span-to-depth were 2.0 and 2.5 respectively, the failure modes were flexure-shear failure mode, which were very close to the flexural failure mode as illustrated in Fig. 6. However, with the contribution of the encased steel shape, the failure modes of all seven specimens were not as brittle as that of the reinforced concrete beams, especially in the specimens CPSRC-5 and specimen CPSRC-6, whose failure modes were very ductile.

It could be also observed that the failure modes of the specimen CPSRC-2 and specimen CPSRC-4 beam specimens were almost as same as that of the specimen CSRC-7, which had the same dimensions and shear span-to-depth ratios. They all failed in similar failure mode as illustrated in Fig. 6. Furthermore, after the test, a couple of the specimens were cut open, which was illustrated in Fig. 7, there were not any slippage found on the interface between the steel shape and the concrete and it was difficult to distinguish the precast outer-part from the cast-in-place

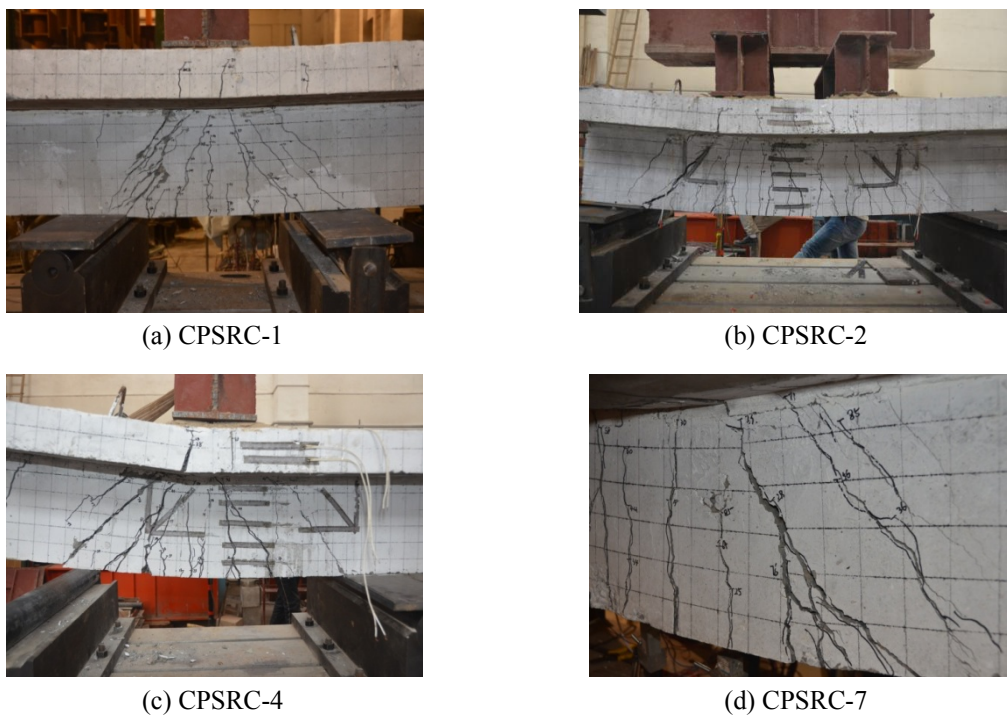


Fig. 7 Specimens failed in shear compression failure

part. It also revealed that no local buckling of the steel shapes had taken place from the cut-open specimens, but a corner of the hole in the steel shape was torn apart at the tension zone.

3.2 Shear force-curvature curves

Fig. 8 shows the shear force-curvature curves of the specimens, the curvatures were calculated by dividing the deflection value to the length of the shear span. From the shear force-curvature curves of specimens, it could be found that all the specimens behaved ductile, even the specimens whose shear span-to-depth ratio was low to 1.0. And also from these curves, it could be observed that there was not obvious difference in stiffness of all the specimens.

From the shear force-deflection curves, the ductility ratios of specimens were calculated as listed in Table 2. Here, the ductility ratio was defined as the result of the ultimate load-point deflection Δ_u divided by the yielding load-point deflection Δ_y , and the ultimate load-point deflection Δ_u was defined as the curvature of the specimen when its load right descended to 85



Cut-open photo of CPSRC-7

Fig. 8 Specimens failed in flexural shear failure

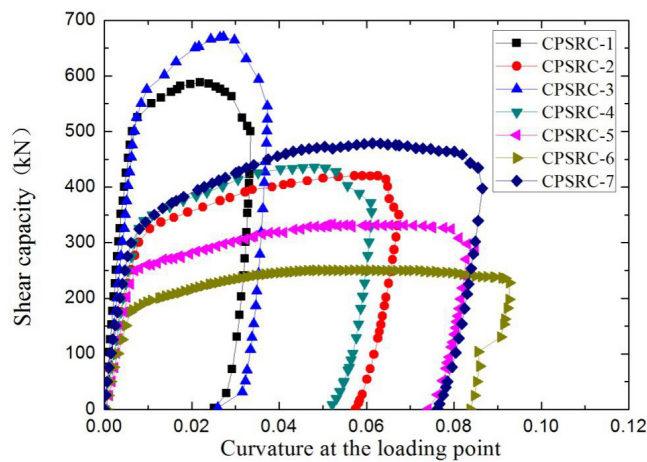


Fig. 9 The shear force-curvatures of the specimens

percent of the peak load during the failing stage. And the yielding load-point deflection Δ_y was calculated from the test shear force-deflection curves of the specimen and based on a recommended method. From the calculated ductility ratios listed in Table 2, it could be found that, all ductility ratios of the specimens were all higher than 3, which showed good ductility.

4. Shear capacity and discussions

From the measured data and the tested shear force-curvatures of the specimens, the results of the shear capacities of the specimen were obtained and listed in the Table 2. And from these results, the influences or effects of some factors on the shear capacity were found and discussed as follows in this section.

4.1 effect of concrete strength

As well known, the concrete strength plays an important role on the shear capacity of the reinforced concrete beams as well as steel reinforced concrete beams. But in steel reinforced concrete beams, the concrete contributed fewer portions than in reinforced concrete because the web of the steel shape bears large portion of the shear force. In this test, for the specimen CPSRC-1 to CPSRC-7 the concrete strength of the precast outer-part was all the same, but the concrete in the cast-in-place inner part were varied. For the specimen CPSRC-2, CPSRC-4 and CPSRC-7 which had the same shear span-to-depth ratios, the concrete strength of the inner concrete was 21.7 MPa, 38.1 MPa and 68.0 MPa, and the tested shear capacities of them were 420 kN, 435 kN and 480 kN, respectively. Thus, it could be observed that the concrete strength directly affected the shear capacity, and the shear capacity of the specimen increased proportionally to the increasing of the concrete strength, as illustrated in Fig. 9.

4.2 effect of shear span-to-depth ratio

Fig. 10 showed the relation curves of the shear span-to-depth ratio vs. the shear capacity of the specimens. From Fig. 10, it could be seen the shear capacity of the specimen was heavily affected by the shear span-to-depth ratio. For instance, the shear capacities of the specimen CPSRC-3,

Table 2 Test results of the specimens

Specimen ID	Load of the first cracking P_{cr} (kN)	Load of the steel yielding P_y (kN)	Peak load P_u (kN)	Shear capacity V_u (kN)	Yielding deflection Δ_y (mm)	Ultimate deflection Δ_u (mm)	Ductility ratios Δ_u/Δ_y
CPSRC -1	230	1050	1170	585	2.83	12.39	4.37
CPSRC -2	130	718	840	420	11.67	37.62	3.22
CPSRC -3	270	1170	1340	670	3.70	13.97	3.77
CPSRC-4	160	729	870	435	8.29	34.23	3.83
CPSRC-5	96	546	664	332	13.04	63.51	4.87
CPSRC-6	50	429	500	250	18.07	86.56	4.79
CPSRC-7	190	800	960	480	12.67	48.58	3.83

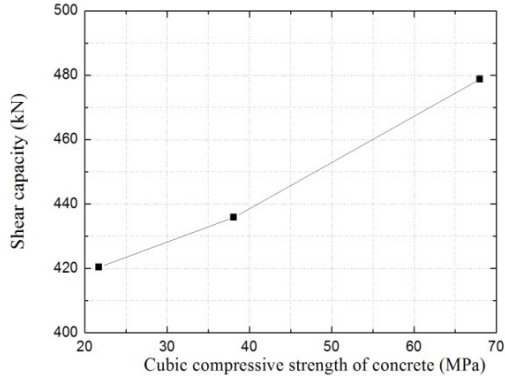


Fig. 10 Shear capacity vs. concrete strength curves

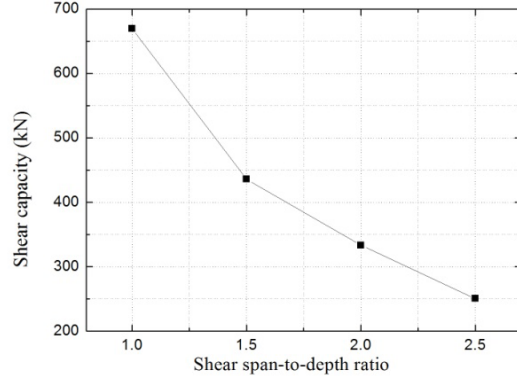


Fig. 11 Shear capacity vs. shear span-to-depth ratios curves

CPSRC-4, CPSRC-5 and CPSRC-6, which were identical in all dimensions and material parameters, the shear span-to-depth ratios of them were 1.5, 1.0, 2.0 and 2.5, the shear capacities were 670 kN, 435 kN, 332kN, and 250kN respectively. The specimen CPSRC-1, CPSRC-2 followed the same trend. From above, it could be observed that the shear capacity of the PSRC beams decreased proportionally to the increasing of the shear span-to-depth ratios in the ranges of 1.0 to 2.5.

4.3 Calculation methods and validation

In the design specifications of SRC structures in China, the shear capacity of the SRC beam with holes in steel web was suggested to be calculated by using formula (1), where λ is the shear span-to-depth ratio, f_t is axial tensile strengths of concrete, b is the web width of the beams, h_0 is the distance from extreme compression fiber to centroid of longitudinal tension reinforcement, t_w is the thickness of the steel shape web, h_w is the height of the steel shape web, f_y is the yield strength of the reinforcement bar, f_{yv} is the yield strength of the shear reinforcement bar, A_{sv} is the area of shear reinforcement within spacing S . S is the center-to-center spacing of shear reinforcement. D_h is the overall height of opening.

$$V_{c,SRC} = \frac{1.75}{\lambda + 1.0} f_t b h_0 + \frac{(h_w - D_h) t_w f_y}{\sqrt{3}} + \frac{f_{yv} A_{sv}}{s} h_0 \quad (1)$$

In Eq. (1), the effect of the shear span-to-depth ratios and effect of the concrete strength were both considered, but the effect of the flange of the T-beam was not taken into account. For CPSRC beam proposed in this paper, there are two kinds of concrete in the beam, and therefore a combination tension strength of two kind of concrete named $f_{t,com}$ was used, which could be calculated by using Eq. (2), where A_{c1} , A_{c2} is the area of cast-in-situ concrete and precast concrete in rectangular cross section beams, f_{t1} , f_{t2} is the axial tensile strengths of cast-in-situ concrete and precast concrete, which were illustrated in Fig. 11, and could be calculated by using formula (3).

$$f_{t,com} = \frac{A_{c1}}{A_{c1} + A_{c2}} f_{t1} + \frac{A_{c2}}{A_{c1} + A_{c2}} f_{t2} \quad (2)$$

$$f_t = 0.26f_{cu}^{2/3} \tag{3}$$

And then the shear capacity of CPSRC beams without flange in the compression zone could be calculated by using Eq. (4). For the CPSRC beams with flange in the compression zone, which were specimens of series A in this paper, a coefficient γ'_f was introduced to take the effect of the flange into account, and then Eq. (5) was suggested to calculate their shear capacity. The coefficient γ'_f was supposed to be a variable and be affected by a couple of parameters, and it was proposed be calculated by using Eq. (6), where b'_f is the slab width of the beams, h'_f is the slab height of the beams. Based on the calculation methods and formulas established above, the shear capacities of the specimens were calculated and listed in Table 3.

$$V_{c,SRC} = \frac{1.75}{\lambda + 1.0} f_{t,com} b h_0 + \frac{(h_w - D_h) t_w f_y}{\sqrt{3}} + \frac{f_{yv} A_{sv}}{s} h_0 \tag{4}$$

$$V_{c,CPSRC} = \frac{1.75(\gamma'_f + 1.0)}{\lambda + 1.0} f_{t,com} b h_0 + \frac{(h_w - D_h) t_w f_y}{\sqrt{3}} + \frac{f_{yv} A_{sv}}{s} h_0 \tag{5}$$

$$\gamma'_f = \frac{(b'_f - b) h'_f f_{c1}}{A_{c1} f_{c1} + A_{c2} f_{c2}} \tag{6}$$

From the results listed in Table 3, it can be seen that the calculated shear capacities of specimens were close to the experimental results, especially for the specimens whose shear span-to-depth ratios were larger than 1.0 and less than 2.5, the calculated results of which were very close to the experimental results. But for the specimen CPSRC-1 and specimen CPSRC-3 whose shear span-to-depth ratios were 1.0, the calculated shear capacities were smaller than the experimental results. And for the specimen CPSRC-6, whose shear span-to-depth was 2.5, the calculated shear capacities of them were larger than the tested shear capacities. Therefore, for the specimens whose shear span-to-depth ratios were among the range from 1.5 to 2.5, the proposed formula can be used to calculate the shear capacity. But for the specimens whose shear span-to-

Table 3 Comparisons of the calculated results of shear capacities of the specimens

Specimen ID	A_{c1} (mm ²)	f_{t1} (MPa)	A_{c2} (mm ²)	f_{t2} (MPa)	V_u (kN)	V_c (kN)	V_c/V_u
CPSRC-1	45200	2.76	34800	3.71	585	401	0.69
CPSRC-2	45200	2.76	34800	3.71	420	344	0.82
CPSRC-3	45200	3.27	34800	3.71	670	486	0.73
CPSRC-4	45200	3.27	34800	3.71	435	412	0.95
CPSRC-5	45200	3.27	34800	3.71	332	362	1.09
CPSRC-6	45200	3.27	34800	3.71	250	326	1.30
CPSRC-7	45200	3.98	34800	3.71	480	505	1.05
Average value							0.95
coefficient of variation							0.23

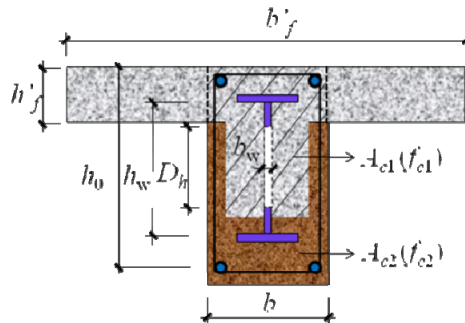


Fig. 12 Shear capacity calculation parameters diagram

depth ratios were smaller than 1.5, especially were smaller than 1.0, the proposed formula will be little conservative, and some other calculation methods such as strut-and-tie modeling methods should be introduced. And for the specimens whose shear span-to-depth ratios were larger than 2.0, which were supposed to fail in flexural-shear failure mode, the capacities should be calculated with more consideration of the effect of bending moment.

5. Conclusions

A new developed partially precast castellated steel reinforced concrete beam, which is abbreviated as CPSRC beam, has been proposed and introduced. With a series of experiments of seven CPSRC T-beam specimens, the shear performance of such kind of CPSRC beams that worked under sagging moment has investigated. Based on the observation and the discussion of the experimental results, the following conclusions can be drawn as follows:

The performance of CPSRC beam specimens was similar to the wholly cast-in-place SRC specimens. For the specimens whose shear span-to-depth ratios were smaller than 2.0, the specimens failed in typical shear compression shear failure modes and damages patterns. And For the specimen whose shear span-to-depth ratios were 2.0 and 2.5, the failure modes were flexure-shear failure mode. However, with the contribution of the encased steel shape, the failure modes of all seven specimens were not as brittle as that of the reinforced concrete beams.

The shear capacities of the CPSRC beams were directly affected by the concrete strength, and the shear capacities increased proportionally with the increasing of concrete strength.

The shear capacities of the CPSRC beams were also directly affected by the shear span-to-depth ratios of specimens, and the shear capacities decreased proportionally to the increasing of shear span-to-depth ratios, which were within the range of 1.0 to 2.5.

A set of calculation method of the shear capacity of the CPSRC beam was proposed and introduced, with the comparison of the calculated results based on this proposed method to the experimental results, the proposed method was verified to be valid.

Acknowledgments

The experiments were sponsored by the National Natural Science Foundation of China (Program No.51478287 and No.51578443), Shaanxi Province National Science Foundation

(Program No. 2015JM5187) and were also supported by the Program for Changjiang Scholars and Innovative Research Team at the University of China as well as the Program for Innovative Research Team of Xi'an University of Architecture and Technology.

References

- Chen, S. and Jia, Y. (2008), "Required and available moment redistribution of continuous steel-concrete composite beams", *J. Constr. Steel Res.*, **64**(2), 167-175.
- Chen, S.M., Limazie, T. and Tan, J. (2015), "Flexural behavior of shallow cellular composite floor beams with innovation shear connection", *J. Constr. Steel Res.*, **106**, 329-346.
- GB/T 700-2006 (2006), *Carbon Structure Steels*, China Planning Press, Beijing, China.
- GB/T 50081-2002 (2002), *Standard for Test Method of Mechanical Aroperties on Ordinary Concrete*, China Planning Press, Beijing, China.
- Hegger, J., Roggendorf, T. and Kerkeni, N. (2009), "Shear capacity of prestressed hollow core slabs in slim floor constructions", *Eng. Struct.*, **31**(2), 551-559.
- Hong, W.K., Kim, J.M., Park, S.C., Kim, S.I., Lee, S.G., Lee, H.C. and Yoon, K.J. (2009), "Composite beam composed of steel and precast concrete; (Modularized Hybrid System, MHS) Part II: Analytical investigation", *Struct. Des. Tall Spec.*, **18**(8), 891-905.
- Hong, W.K., Park, S.C., Kim, J.M., Lee, S.G., Kim, S.I., Yoon, K.J. and Lee, H.C. (2010), "Composite beam composed of steel and precast concrete; (Modularized Hybrid System, MHS) Part I: Experimental investigation", *Struct. Des. Tall Spec.*, **19**, 275-289.
- Johnson, R.P. (2004), *Composite Structures of Steel and Concrete: Beams, Slabs, Columns, and Frames for Buildings*, Blackwell Publication, USA.
- Lawson, R.M., Lim, J., Hicks, S.J. and Simms, W.I. (2006), "Design of composite asymmetric cellular beams and beams with large web openings", *J. Constr. Steel Res.*, **62**(6), 614-629.
- Leon, R.T. (2004), "Composite construction in steel and concrete V", *Proceedings of the 5th International Conference*, Berg-en-Dal, South Africa, July.
- Leon, R.T. (2008), "Composite construction in steel and Concrete VI", *Proceedings of the 2008 Composite Construction in Steel and Concrete Conference*, Tabernash, CO, USA, July.
- Nie, J., Fan, J. and Cai, S. (2004), "Stiffness and deflection of steel-concrete composite beams under negative bending", *J. Struct. Eng.*, **130**(11), 1842-1851.
- Redwood, R. and Demirdjian, S. (1998), "Castellated beam web buckling in shear", *J. Struct. Eng.*, **124**(10), 1202-1207.
- Yang, Y., Zhou, X., Xue, J. and Huo, J. (2012), "Experimental study on fatigue behavior of composite girders with steel plate-concrete composite decks", *China Civil Engineering Journal.*, **45**(6), 123-113. [In Chinese]